Available online at www.sciencedirect.com
SCIENCE DIRECT®
Polymer 45 (2004) 275–286
polymer
www.elsevier.com/locate/polymer

Toughening of polypropylene by combined rubber system of ultrafine full-vulcanized powdered rubber and SBS

Yiqun Liu[a], Xiaohong Zhang[a], Jianming Gao[a], Fan Huang[a], Banghui Tan[a], Genshuan Wei[b], Jinliang Qiao[a,*]

[a]*Plastic Processing Center, SINOPEC Beijing Research Institute of Chemical Industry, North Third Ring Road 14, Beijing 100013, People's Republic of China*
[b]*Institute of Applied Chemistry, College of Chemistry and Molecular Engineering, Peking University, Beijing 100080, People's Republic of China*

Received 11 July 2003; received in revised form 25 September 2003; accepted 4 November 2003

Abstract

A combined rubber system of ultrafine full-vulcanized powdered rubber (UFPR) and SBS was used for polypropylene toughening. The PP toughened with the combined rubber system shows not only higher impact strength as compared to each rubber component used alone but also good stiffness and heat resistance. Crystallization study shows that the UFPR is more efficient in promoting the crystallization of PP than SBS, leading to a higher crystallinity and an enhancement of stiffness and heat resistance of PP. The combined rubber system containing UFPR and a small amount of SBS still possesses a good nucleating ability. Transmission electron microscopy results indicate that the combined rubber system mostly forms an encapsulation structure of UFPR particles encapsulated by SBS phase. This morphology was also confirmed by scanning electron microscopy results through observing the fracture surfaces of toughened samples. A small amount of SBS was found to be helpful for a better dispersion of UFPR in PP matrix. The causes for the encapsulation morphology and the synergistic toughening effect were discussed. A tentative explanation was given by comparison of the solubility parameter of each component in the toughened samples.

Keywords: Polypropylene; Morphology; Toughening

1. Introduction

Polypropylene is the most widely used plastics for general purpose, the toughening study of which has always been very important in polymer blending area. A lot of research papers are published each year concerning the toughening of PP. Although many approaches have been used to toughen PP, the most effective ways are still the conventional ones, that is, using rubbers or elastomers. But this will cause deterioration in stiffness and heat resistance though the toughness is increased.

In our previous paper [1], a new powdered rubber for PP toughening was introduced. It can improve the toughness of PP greatly while increasing its stiffness and heat resistance, which makes the toughened PP possess a balanced toughness and stiffness. We called this rubber toughener elastomeric nano-particle (ENP), or ultrafine full-vulcanized powdered rubber (UFPR) [1–3]. This UFPR was prepared by irradiating rubber latex, used as raw material, and spray drying it. Various UFPRs can be prepared from a selection of different rubber latexes. We have prepared several UFPRs by using this proprietary method [4] and employed them in various plastics for plastic toughening and preparing thermoplastic vulcanizates [1–7].

For PP toughening, a UFPR with nucleator was obtained by dissolving in water sodium benzoate, a common nucleator of PP, mixing it with rubber latex, and co-spray drying the mixture. Since the sodium benzoate is mixed with rubber latex particles in solution form, it will compound with rubber particles as water evaporates during the spray drying process. Therefore, the UFPR can be obtained with each particle uniformly compounded with nucleator. This UFPR has prominent effect on toughening, stiffening and improving heat resistance of PP. A common PP nucleator, Sodium benzoate has an inferior nucleation effect to some high efficient nucleators though, it costs low and uses easy

* Corresponding author. Tel.: +86-10-64216131-2375; Fax: +86-10-64228661.
E-mail addresses: jqiao@brici.ac.cn (J. Qiao).

0032-3861/$ - see front matter © 2003 Elsevier Ltd. All rights reserved.
doi:10.1016/j.polymer.2003.11.001

to make each rubber particle uniformly compounded with nucleator by the compounding method mentioned above. Therefore, this method is of great industrial value.

Many rubbers or elastomers, such as EPDM, EPR, SBR, SBS, SEBS, and POE, etc. have been used for rubber toughening PP [8–20]. These PP tougheners were mostly used alone [8–13], or used together with inorganic particles [14–20]. Researches on toughening PP with combined rubbers are seldom reported. Phadke and De [21] had reported using a masterbatch of cryo grounded rubber (CGR) and natural rubber to toughen PP. Their study showed that the toughening effect obtained by using combined rubbers was better than using CGR alone, but no toughening data compared with natural rubber at same loading content was given.

Based on the previous researches of UFPR toughening PP, the authors of this paper attempted to combine two rubber components of UFPR and SBS together for PP toughening, and the toughening effect was better than using single rubber component. Therefore, by studying the morphology of rubber components in PP matrix, the effect of rubbers on the crystallization behavior of PP and so on, the authors of this paper try to find out the differences between the combined rubber system and single rubber component in affecting the mechanical properties of PP, and the causes for synergistic toughening effect brought about by the use of combined rubber system.

2. Experimental section

2.1. Materials and sample preparation

Materials used in this study were: polypropylene homopolymer PP-A, MFR, 0.24 g/10 min, made by Daqinghuake Corp., China; polypropylene homopolymer PP-B, B-200, MFR, 0.2 g/10 min, commercially produced by SINOPEC Luoyang PetroChem., China; styrene butadiene UFPR, Narpow™ VP-101 (average single particle size, ca 100 nm; T_g, −25.4 °C; gel fraction 88%; containing 10 phr sodium benzoate; molar ratio of styrene/butadiene, 50/50; density, 1.0 g/cm^3), manufactured by Beijing BHY Chemical Industry New Technology Company, China; and styrene–butadiene–stryrene elastomer, SBS 1401, commercially produced by SINOPEC Yanshan PetroChem., China.

Melt blending was carried out on a co-rotating twin screw extruder (ZSK-25, Werner and Pfleiderer) at a barrel temperature of 180–200 °C and a screw speed of 350 rpm. 0.5 wt% Irganox 1010 and Irgafos 168 (weight ratio 1/1) were added as stabilizers during melt processing. The extruded materials were injection molded to obtain specimens for various mechanical tests with the following specifications: tensile strength test (GB1040-92, $170 \times 10 \times 4$ mm^3) impact strength test (GB1843-93, $127 \times 12.7 \times 6.4$ mm^3), flexural strength test (GB9341-2000, $120 \times 10 \times 4$ mm^3), and heat distortion temperature (HDT) test (GB1634-79, $120 \times 10 \times 4$ mm^3). The barrel and nozzle temperatures of injection-molding machine were 220 and 240 °C, respectively. The same melt blending and injection molding conditions were used throughout the study.

2.2. Experimental measurements

2.2.1. Mechanical properties

Tensile tests were carried out on dumb-bell shaped specimens with an AG-1 tensile machine (50 mm/min, GB1040-92). The notched Izod impact strength was measured by using a CEAST impact machine according to GB1843-93. The flexural strength and modulus tests were carried out on an Instron testing machine (Model 4466) in accordance with GB9341-2000. HDT was tested with a HD-PC Heat Distortion Tester according to GB1634-79.

2.2.2. Morphology observation

The morphology of PP and rubber blends was observed by using transmission electron microscopy (TEM) and scanning electron microscopy (SEM). TEM experiment was performed on a Hitachi 100 transmission electron microscope. The ultrathin sections, 50–100 nm in thickness, were cryotomed from injection molded specimens at −100 °C. Contrast enhancement was achieved by staining the ultrathin sections with an aqueous solution of OsO_4.

Fracture surfaces of specimens obtained from notched Izod impact test were characterized by SEM. The surfaces were sputter-coated with a thin gold layer and studied by using a Philips XL-30 ESEM. In some cases, the fracture surfaces were etched by toluene for 24 h to remove the soluble SBS phase.

2.2.3. Crystallization behavior

Differential scanning calorimetry (DSC) and polarized light microscopy (PLM) were used to study the crystallization behavior of PP blend.

DSC measurements were carried out on a Thermal Analysis Q100 following this procedure: samples were heated to 230 °C and kept isothermal for 5 min to eliminate any thermal history of the material, and then cooled to 40 °C at a rate of 10 °C/min; held for 1 min at 40 °C, the samples were then heated to 200 °C at a heating rate of 10 °C/min. The information obtained from DSC included: the crystallization peak temperature (T_c), the heat of crystallization (ΔH_c), the melting peak temperature (T_m), the heat of fusion (ΔH_f), and the degree of undercooling ($T_m - T_c$).

The formation of spherulite in PP blend was characterized in situ on a hot stage (Linkam Scientific Instruments THMSG 600) using an optical microscope (Leica DMLP) under cross-polarization light. The samples subjected to PLM characterization were prepared as follows. A small piece of sample cut from injection mold bars was sandwiched between two cover-glasses, and then placed

on the hot stage preheated at 230 °C for 1–2 min until the small section melted, followed by pressing the melted sample carefully to form a thin layer. The measurement steps were as follows. The prepared sample was heated at 230 °C for 5 min and then cooled to 110 °C at a rate of 10 °C/min. When the temperature approached 140 °C, PLM images were started to be captured from video signals at a rate of 3–5 s per image.

3. Results and discussion

3.1. Mechanical properties

The data listed in Table 1 show that PP-A1, i.e. the sample toughened with 5 phr UFPR, has much higher impact strength than pure PP (PP-A), as well as higher flexural strength, modulus and HDT. However, in PP-A3, the sample toughened with 5 phr SBS, only the toughness is improved, and is inferior to that achieved by using UFPR, while the stiffness and HDT of PP are decreased. When UFPR and SBS are combined at a weight ratio of 4/1, the sample toughened with this combined rubber system shows clearly a higher impact strength than each single component does at the same loading content, i.e. a synergistic toughening effect, while the deterioration of stiffness and HDT are avoided. As for another PP homopolymer, PP-B, a similar synergistic toughening effect was also found when the PP was toughened with combined rubbers of UFPR and SBS at a ratio of 3/2. These results indicate that toughening with UFPR/SBS combined rubber system is very effective in further increasing toughening effect and achieving an ideal balance of toughness and stiffness. In order to better understand the synergistic effect of the combined rubber system on the impact strength, it is quite necessary to thoroughly investigate the microscopic morphology of toughened PP samples and make clear the dispersion situation of each rubber component in the PP matrix. The PP-A series samples were chosen for an in-depth investigation.

3.2. Morphology of the rubber phase

3.2.1. TEM results

In light of two rubber components in PP matrix when using the combined rubber system, it is very important to clearly differentiate each component for better understanding their dispersion. OsO_4 was used to stain the ultrathin sections for TEM in this study, and it cannot stain the styrene block in SBS. Therefore, the black and white alternative microphase separation structure of SBS can be found under TEM at a high magnification. The styrene butadiene UFPR was obtained via free radical polymerization, the styrene segment of which is evenly distributed in molecular chains. The stained UFPR particles should have homogenous structure under TEM observation due to its molecular structure. Therefore, each rubber component in the combined rubber system can be readily differentiated on TEM micrographs.

As shown in the TEM micrographs of Fig. 1, there are many big particles, i.e. the aggregates of UFPR particles, in PP-A1. The number of big particles is less in PP-A2 at the same magnification (×3000), while the number of small ones and the total number of particles are much more than that in PP-A1. The SBS particles in PP-A3 (Fig. 1(e)) have a wide distribution in size, consisting of some particles larger than 1 μm as well as a great number of small ones of tens of nanometer. The microphase separation structure of SBS can be clearly observed both in big and small particles at a magnification of 40,000 (Fig. 1(f)). It can be found in PP-A2 (Fig. 1(d)) that the particles with ca 100 nm in size also have obvious black and white alternative structure in their exterior parts. On the contrary to pure small SBS particles with white color in center, the center parts of particles in PP-A2 are solid and dark, which demonstrates that the small particles in PP-A2 have a microstructure with UFPR particles located in center and encapsulated mostly by SBS phase outside.

The results from TEM micrographs show that the styrene butadiene UFPR disperses not very well in PP matrix although it has good toughening effect. The UFPR particles made from vulcanized rubber latex have a real diameter of

Table 1
Mechanical properties of pure PP and rubber toughened samples

Sample code	Composition: PP-A/UFPR/SBS	Tensile strength (MPa)	Elongation at break (%)	Notched Izod impact strength (J/m)	Flexural strength (MPa)	Flexural modulus (GPa)	Heat distortion temperature (°C)
PP-A	100/0/0	36.8 ± 0.1	116 ± 12	287 ± 4	33.6 ± 0.3	1.44 ± 0.06	109.6 ± 0.4
PP-A1	100/5/0	36.0 ± 0.2	146 ± 23	470 ± 8	35.1 ± 0.1	1.54 ± 0.03	117.2 ± 0.2
PP-A2	100/4/1	36.3 ± 0.2	128 ± 15	582 ± 29	34.4 ± 0.2	1.52 ± 0.01	118.5 ± 0.1
PP-A3	100/0/5	34.6 ± 0.1	172 ± 36	444 ± 10	31.0 ± 0.5	1.34 ± 0.02	107.5 ± 1.0
	PP-B/UFPR/SBS						
PP-B	100/0/0	37.0 ± 0.1	187 ± 44	288 ± 8	34.5 ± 0.3	1.52 ± 0.01	113.9 ± 0.1
PP-B1	100/5/0	36.8 ± 0.1	142 ± 21	479 ± 8	36.8 ± 0.6	1.62 ± 0.06	120.0 ± 0.1
PP-B2	100/3/2	36.2 ± 0.2	162 ± 31	729 ± 112	36.8 ± 0.2	1.61 ± 0.03	119.4 ± 0.4

ca 100 nm, however, the atomized drops of rubber latex formed through our spray drying process are actually big in size, about 5–15 μm. These drops contain a large number of small rubber particles with 100 nm in size, which will form aggregates after water evaporates. Nevertheless these small particles contained in the aggregates have highly crosslinked structure. They can be separated by strong shear force, while the uncrosslinked particles cannot. For instance, the single UFPR particle, not aggregated ones, can be observed by emulsifying the water dispersion of UFPR powder with high speed emulsifier then observing the dispersed particles in clear liquid layer by means of electron microscope. We also use this method for measuring the particle size of UFPR.

In some other resin systems, such as epoxy resin, nylon, etc. UFPR can be dispersed quite well in the resin matrix, which was believed to relate with the strong interaction or some reactions between these UFPRs and the matrices [2,3]. As for PP, although the styrene butadiene UFPR has lower polarity compared with other polar UFPRs such as

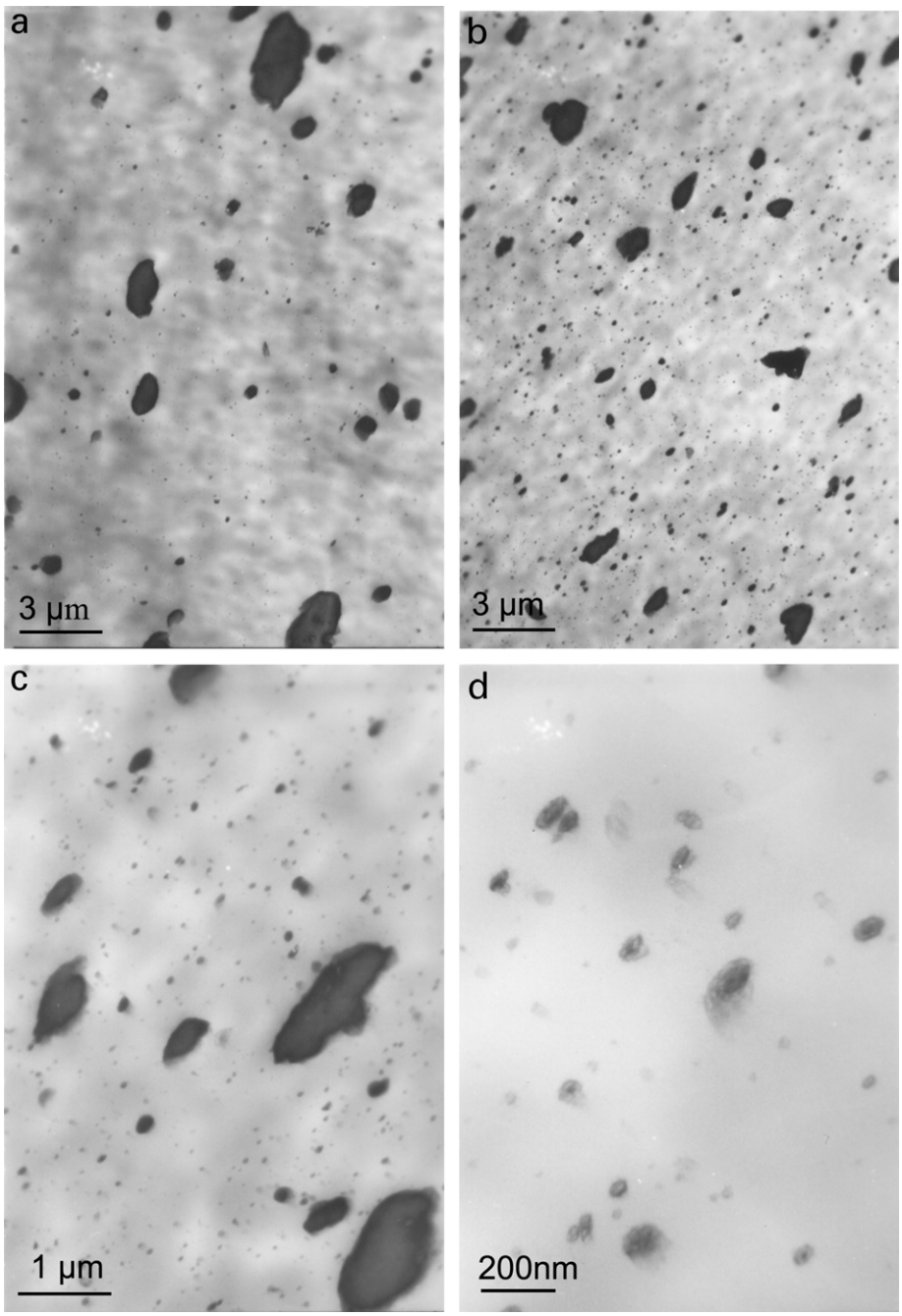

Fig. 1. TEM micrographs of rubber toughened PP samples: (a) PP-A1 ×3000, (b) PP-A2 ×3000, (c) PP-A2 ×10,000, (d) PP-A2 ×40,000, (e) PP-A3 ×10,000, and (f) PP-A3 ×40,000.

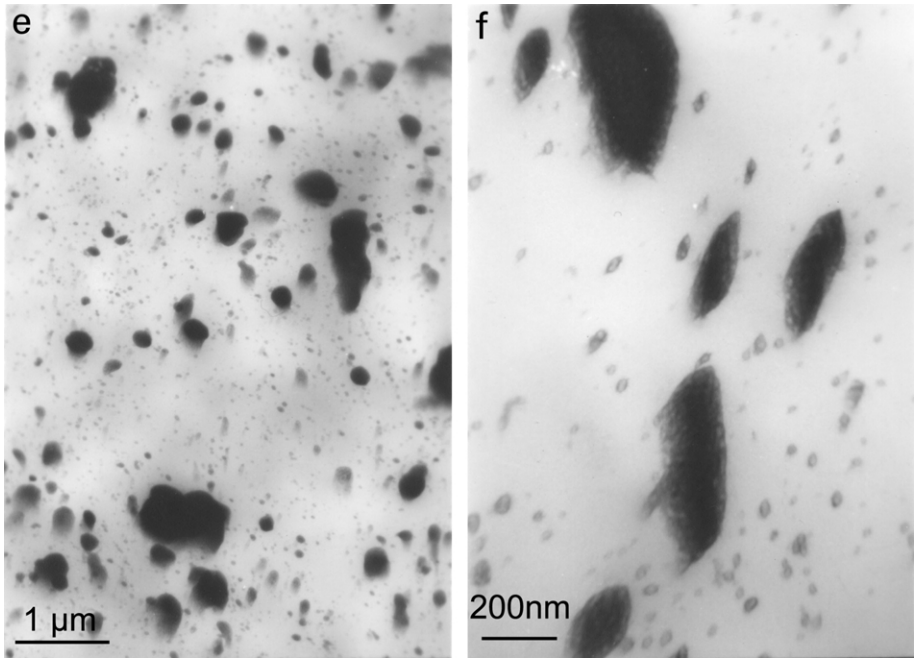

Fig. 1 (*continued*)

acrylonitrile butadiene, carboxylic styrene butadiene, acrylate rubber and, etc. it still has poor compatibility with PP and will not have any interaction or reaction with PP. So it is quite difficult to achieve ideal dispersion of styrene butadiene UFPR in PP matrix. If the dispersion problem can be further solved, and single particle dispersion can finally come true, the toughening effect of UFPR still has potential to be greatly improved. The TEM results just reveal that the incorporation of SBS is effective to help the UFPR aggregates to disperse better.

3.2.2. SEM results

Besides TEM study for rubber morphology, SEM measurements were also used to investigate the fracture surfaces of various PP samples. As shown in Fig. 2, a lot of convex particles and concave holes exist on the fracture surfaces of PP-A1 and PP-A2. The formation of these particles or holes should be related to the separation or pullout of UFPR aggregates from PP matrix during the impact test. Detailed discussion of the fracture morphology and toughening mechanism will be published in another paper. The fracture surface of PP-A3 (see Fig. 2(d)) differs obviously from those of UFPR toughened samples in that no convex particles or concave holes can be found on their fracture surfaces. However, a lot of holes can be observed on the fracture surface after PP-A3 was etched by using toluene to dissolve the SBS phase. The size and distribution of these holes are similar to those of SBS phase as observed in TEM. The morphology that interests us more is that the edges of many convex particles in PP-A2 sample were etched off after etching as shown in Fig. 2(c). This phenomenon reveals that these convex particles are surrounded by SBS phase, since UFPR particles with highly crosslinked structure cannot be dissolved in toluene. This result agrees well with that of TEM observation, and strongly confirms that the combined rubber system of SBS and UFPR will form a special morphology in PP matrix, i.e. an encapsulation structure with UFPR particles surrounded or partly surrounded by SBS phase.

3.3. Effect of rubber on the crystallization of PP

It can be seen from the comparison of mechanical data that the PP samples toughened with UFPR or UFPR/SBS combined rubber system have higher stiffness and HDT than pure PP, while the sample toughened with single SBS component has lower stiffness and heat resistance than the samples containing UFPR component and even the pure PP. According to previous study on crystallization kinetics [1], it was believed that the UFPR containing nucleator has nucleation effect on PP and promotes its crystallization, and thus increases its stiffness and heat resistance. It was also shown in some literature about rubber toughening PP [8–10] that rubber toughener such as EPDM or SBS has nucleation effect and can increase the crystallization temperature and decrease the size of spherulite. These researches all indicate rubber has some nucleation effect, but the differences in stiffness and heat resistance of PP samples toughened with different rubbers as given in Table 1 reflect the differences in these rubbers. We thus study these differences by comparing the influences of UFPR and SBS on crystallization behavior of PP from different aspects through DSC and PLM methods.

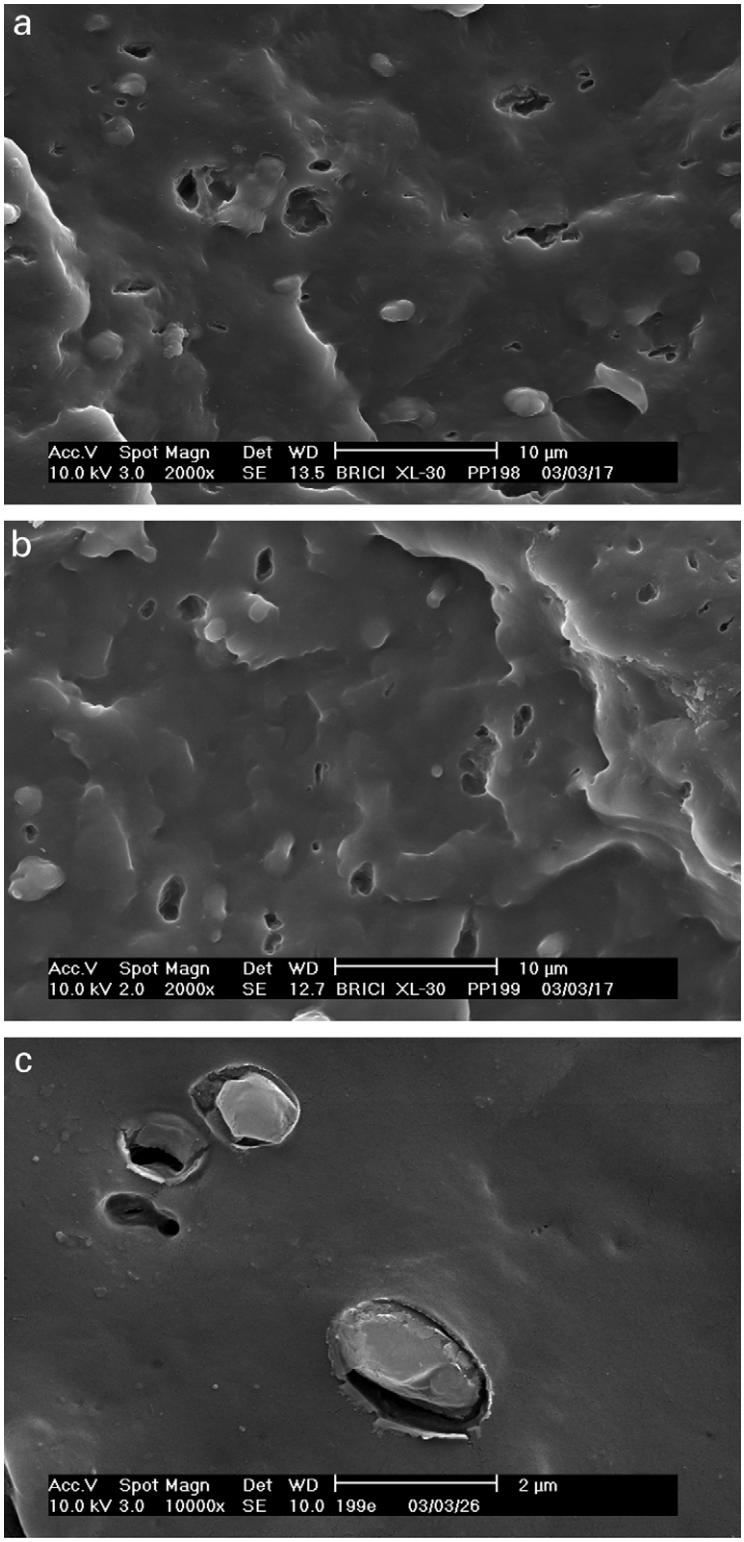

Fig. 2. SEM micrographs of the fracture surface of rubber toughened PP samples: (a) PP-A1, (b) PP-A2, (c) PP-A2 (after etching), (d) PP-A3, and (e) PP-A3 (after etching).

3.3.1. DSC results

The crystallization temperatures listed in Table 2 show that all the rubber toughened samples that have higher crystallization temperatures than pure PP, and the samples containing UFPR, i.e. PP-A1 and PP-A2, are more prominent in increasing the crystallization temperature than the sample toughened with SBS, PP-A3. These results indicate that the incorporation of rubber has nucleation

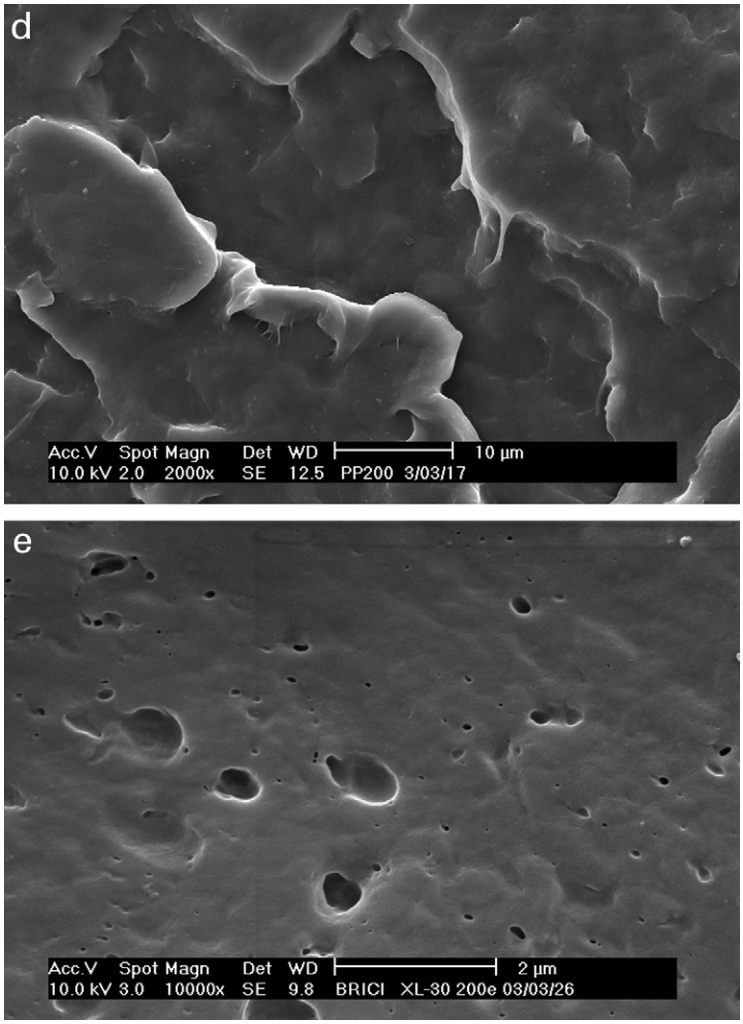

Fig. 2 (*continued*)

effect on PP and thus results in the increase of crystallization temperature of PP. Moreover, UFPR is compounded with nucleator and thus has more obvious nucleation effect than SBS. A small amount of SBS combined with UFPR, compared to pure UFPR, has little difference in affecting the PP crystallization. The melt temperatures of rubber toughened samples are all slightly higher than that of pure PP, nevertheless the undercooling data show a decrease after the incorporation of rubbers due to a great increase in the crystallization temperature.

The crystallization heat and fusion heat can reflect the difference in crystallinity of various samples. The data in Table 2 show that PP-A1 and PP-A2 are basically same in the crystallization heat but higher that of pure PP, while

Table 2
DSC data of pure PP and rubber toughened samples

Sample code	Composition: PP-A/UFPR/SBS	Crystallization peak temperature T_c (°C)	Melting peak temperature T_m (°C)	Degree of undercooling $T_m - T_c$ (°C)	Heat of crystallization ΔH_c (J/g)	Heat of fusion ΔH_f (J/g)
PP-A	100/0/0	121.2	162.4	41.2	97.5	99.9
PP-A1	100/5/0	127.5	164.4	36.9	98.8	102.6
PP-A2	100/4/1	127.4	164.3	36.9	98.0	100.9
PP-A3	100/0/5	124.9	164.2	39.3	94.1	96.0

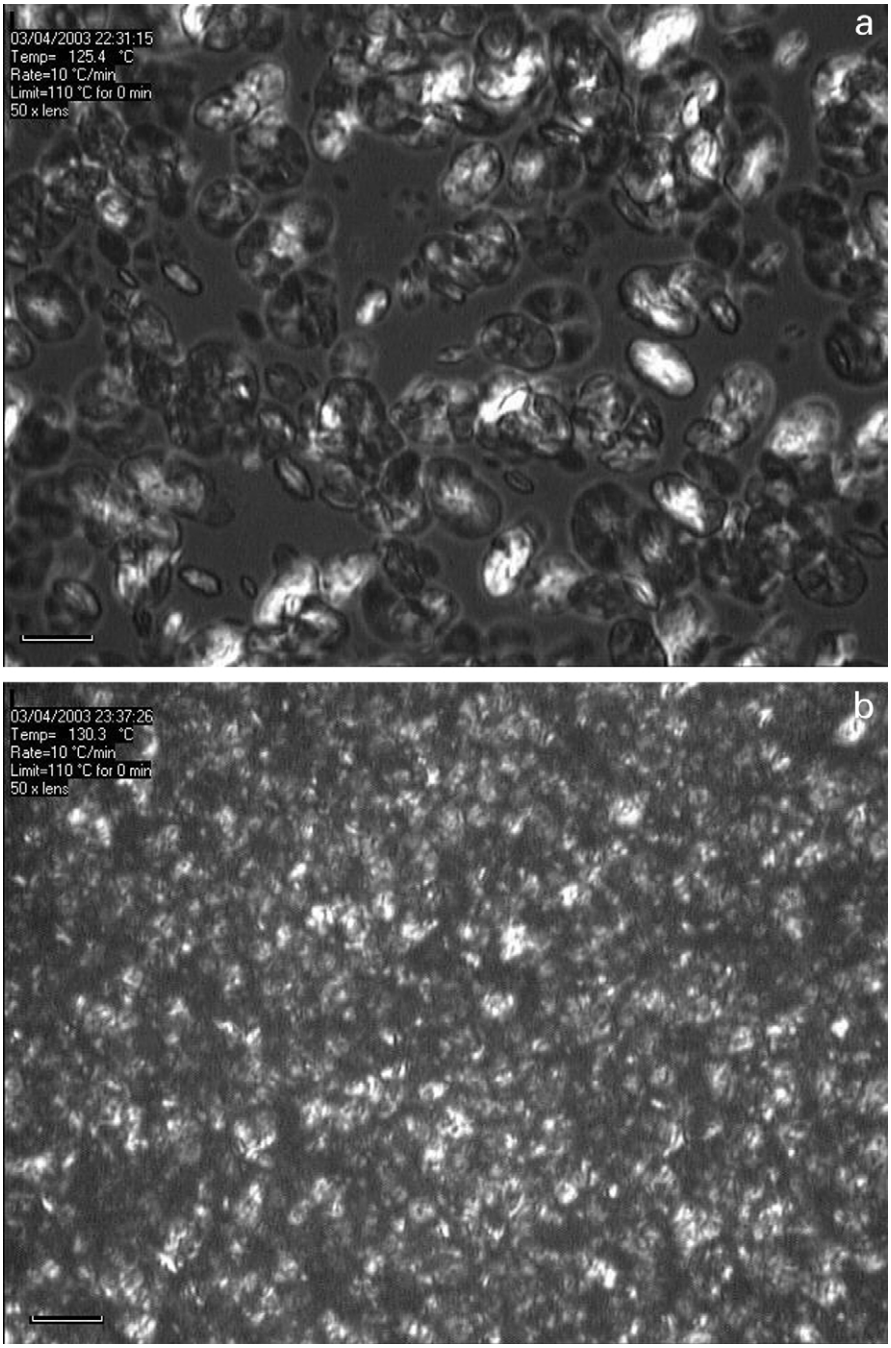

Fig. 3. PLM images of PP samples at different temperatures: (a) PP-A at 125.4 °C, (b) PP-A1 at 130.3 °C, (c) PP-A2 at 129.3 °C, (d) PP-A3 at 123.8 °C. The scale bar in each image stands for 20 microns.

PP-A3 are lower than pure PP. This indicates that UFPR and UFPR/SBS combined rubber system can increase the apparent crystallinity of PP during the crystallization process, while SBS cannot increase the crystallinity though it has some nucleation effect.

3.3.2. PLM results

The appearance of some bright spots is observed in PP-A1 at 133.7 °C in PP-A1 and at 132.8 °C in the rest three samples through in situ characterizing the cooling crystallization by PLM. It follows that the PP samples can nucleate near the above temperatures under the experimental conditions, and the primary nuclei can form earlier for the sample containing 5 phr UFPR. During the cooling process, different samples are found to have different time from the formation of primary nuclei to the growth and collision of spherulites. All the samples are cooled at a same rate, so the PLM images at different temperatures depict the crystallization progress at different time. Since the primary nuclei for all the samples occur at nearly the same

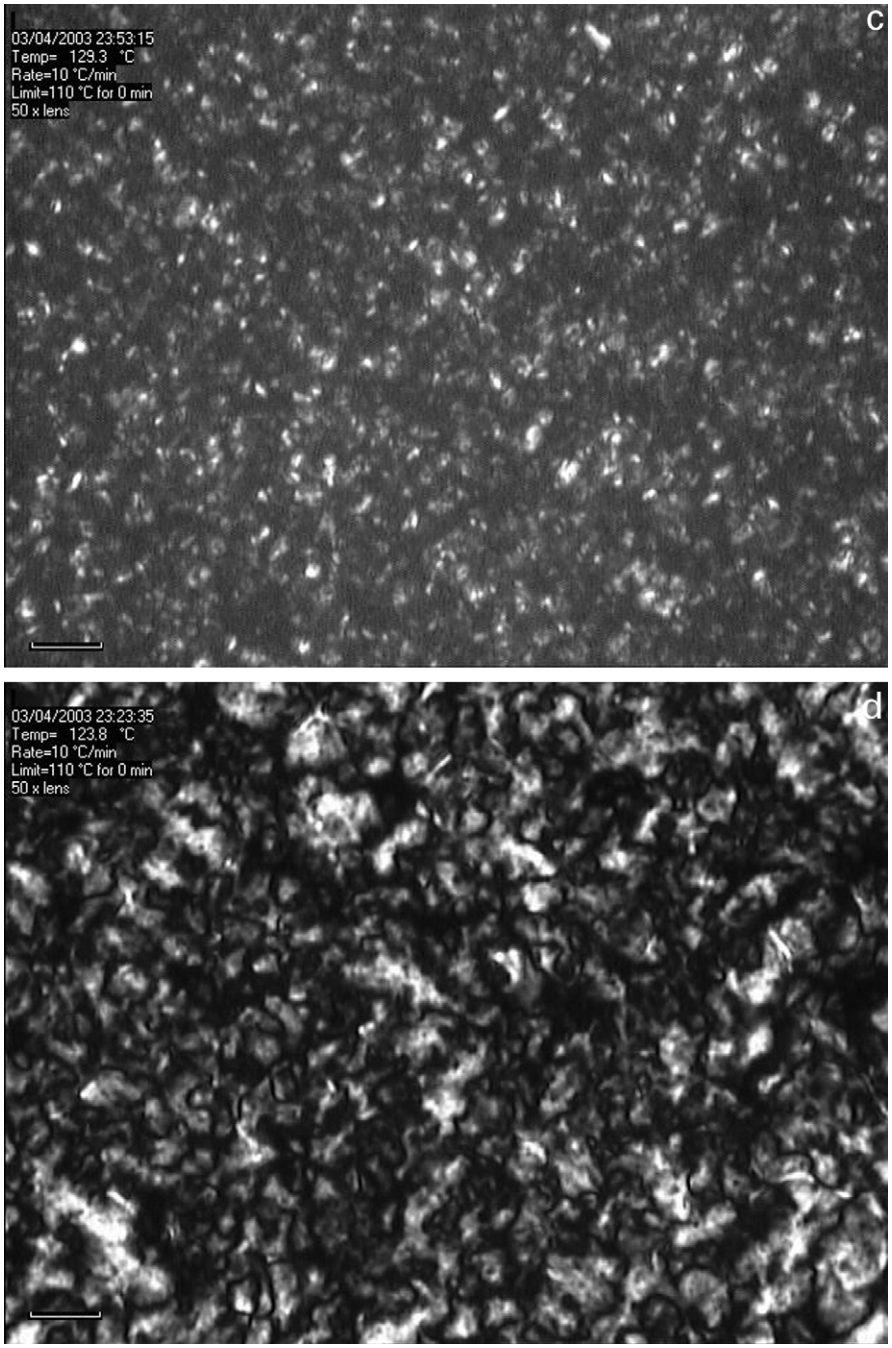

Fig. 3 (*continued*)

temperature, if the collision of spherulites occurs at a lower temperature, then this process takes a longer time and the time left for each spherulite to grow is longer. If the number of nuclei formed during cooling is less, the large spherulites will form.

It should be reminded that a large number of images were captured during cooling process, and only some typical PLM images of crystalline growth were selected and shown in Fig. 3. By comparison of the PLM images captured at different temperatures, it can be found that the collision of spherulites in PP-A occurs at 123.8–121.4 °C. As for PP-A3, the temperature at which spherulites collide is 125.3–123.8 °C. It can also be found that PP-A3 has more nuclei than pure PP and the size of spherulites in PP-A3 is small. The temperatures of collision of spherulites in PP-A1 and PP-A2 are 130.3–129.2 °C and 129.3–128.3 °C, respectively.

The PLM images can directly reflect the nucleation ability of different samples. The sample having strong nucleation ability will form more spherulites with smaller size. It can be seen from the PLM images that the numbers of spherulites in PP-A1 and PP-A2 are clearly more than

that in PP-A3, and pure PP has the least number of spherulites. The toughener in PP-A1, pure UFPR component, contains more nucleator compared with the other samples and thus can form more nuclei, and these nuclei occur earlier than the others. In PP-A2, UFPR component forms smaller UFPR particles containing nucleator with the help of a small amount of SBS. It is difficult for SBS phase to completely encapsulate UFPR particles, therefore a part of nucleator in UFPR has chance to contact with PP matrix, resulting in more nuclei too. As for PP-A3, though it contains a large amount of fine SBS particles, only a part of which have nucleation effect because they contain no nucleator. While PP-A is pure PP, not containing any material with nucleation effect, consequently it has the least number of nuclei and the largest spherulites among all samples.

PLM and DSC experiments are carried out following the same cooling procedure. The different crystallization behavior can be compared through observing the growth of spherulites by PLM, while the heat change during crystallization can be measured by DSC method. Therefore the experimental results of crystallization obtained from different methods can be confirmed by comparing them. The DSC results show that the crystallization temperatures of PP-A1, PP-A2 are higher than those of PP-A3 and PP-A; the PLM results show that the starting temperatures of collision of spherulites in PP-A1 and PP-A2 are higher than those in PP-A3 and PP-A, the sequence of which is consistent with the DSC data of T_c. The crystallization heat of DSC data show that the apparent crystallinity of PP-A1 and PP-A2 are higher than that of pure PP and PP-A3; the PLM results show that the former two samples have more spherulites than the latter ones. It follows that the DSC and PLM results agree well with each other. There is one question here, that is, although SBS has nucleation effect and the number of spherulites in the SBS toughened sample is more than that in pure PP, the crystallization heat of the SBS toughened sample is lower than that of pure PP. It may be explained like this. Although SBS can increase the primary nuclei in PP matrix, it has non-crosslinked molecular structure, which makes the phase separation of SBS particles from PP melt occur gradually when cooling. During the growing of spherulites of PP, i.e. the secondary nucleation process of PP, the arrangement of PP molecules is obstructed by the SBS molecules gradually separated from PP melt, leading to the final imperfect crystalline structure, and the apparent crystallinity decreases.

According to the DSC and PLM results and the aforementioned mechanical data, it is believed that the data corresponding to the stiffness and heat resistance in Table 1 are correlated with the crystallization of PP. In PP-A1, the toughener UFPR has strong nucleation effect and can increase the crystallinity of PP at the same time, which accordingly makes the HDT as well as the flexural modulus and strength higher than those of pure PP. Compared to this, the nucleation effect of SBS is clearly weaker than the nucleator contained UFPR. Although SBS can increase the crystallization temperature of PP, its possible obstruction to the growing of PP spherulites makes the final spherulites imperfect and thus affects the macroscopic mechanical properties, that is, the SBS toughened PP has lower stiffness and heat resistance than those of pure PP. In PP-A2, a small amount of SBS can help the UFPR disperse better in PP matrix, and the crystallization of PP can still be influenced by some nucleators in UFPR particles not completely encapsulated by SBS. Consequently, the combined rubber system has nearly the same nucleation effect as the pure UFPR system, resulting in the good stiffness and heat resistance of the toughened PP.

3.4. Discussion about the encapsulation structure and the synergistic toughening effect

It is known from the study of microscopic morphology that the UFPR/SBS combined rubber system can form an encapsulation structure after blending with PP. This structure is quite similar to the core-shell structure or encapsulation structure reported in some researches of ternary composite system of PP/elastomer/filler [15–20], except for the difference in the core part. Pukanszky et al. [20] had analyzed the cause for the formation of such structure and given a tentative explanation. They made a thermodynamic calculation of the free energy change for the formation of encapsulation structure or the formation of the structure of separate dispersion of filler and elastomer, and found that encapsulation is a thermodynamically favored process. During the calculation, assumptions and numerous approximations were made because of the complexity of ternary system, which may affect the accuracy of calculation. Nevertheless this qualitative analysis is helpful for better understanding the cause for the formation of encapsulation structure.

In the ternary system of PP/elastomer/filler, many experimental results show that the formation of encapsulation structure can be influenced by changing the polarity of the components of the system. For example, Jancar and Dibenedetto [16] had found in the PP/EPR/filler system that the incorporation of maleic anhydride modified EPR in the system can strengthen the interaction between EPR and filler, and can increase the encapsulation structure in the system. In the PP/EPDM/mica system [18], the incorporation of acrylic acid grafted PP can improve the interaction between the organic filler and the matrix, and make it easier to form the structure of separate dispersion of filler and elastomer. Accordingly it is believed that the important factor determining the formation of encapsulation structure is whether the interaction among each component is strong or weak in the system.

In the blend system of our research, there exit no polar inorganic particles, but the compatibility among each component should be different. We can analyze their interaction through calculating the solubility parameter of

each component. According to the data of contribution of each functionality to the cohesive energy and molar volume published by Fedors [22], it can be readily estimated that the solubility parameter of UFPR is 19.98–20.09 $(J/cm^3)^{1/2}$. (The data range are calculated in term of molar ratio of styrene/butadiene being 50/50, the molecular structure of butadiene segment being complete 1,4 structure or complete 1,2 structure). The solubility parameters of SBS and PP are 19.28 and 16.41 $(J/cm^3)^{1/2}$, respectively. (The value of SBS is calculated in term of molar ratio of styrene/butadiene being 70/30, the molecular structure of butadiene segment being complete 1,4 structure). It can be seen that the solubility parameters of UFPR and SBS are close to each other, and the solubility parameter of SBS is between those of UFPR and PP. These solubility parameters reveal that SBS and UFPR have good compatibility, and the former has better compatibility with PP. It should be noted that the polar sodium benzoate in UFPR is not considered in calculation. Therefore the real solubility parameter of UFPR should be much higher than that of SBS, or the compatibility between UFPR and PP differs more obviously from that between SBS and PP.

Although it is not very accurate to estimate solubility parameters by using Fedors' method [23], some other experimental results show us the same compatibility sequence. For instance, Fig. 2(d) shows the fracture surface of PP sample toughened with SBS alone, where no convex particles and concave holes can be observed. This morphology is quite different from the fracture morphology of PP toughened with UFPR component, which has a large number of convex particles and concave holes on the fracture surface. When etching the fracture surface of SBS toughened PP sample, many holes left on the surface can be clearly observed as SBS was etched off. This phenomenon indicates that SBS has better compatibility with PP than UFPR has.

Since the solubility parameter of each component is different and the compatibility among each other differs too, the morphology and dispersion of each component during melt blending will be influenced by these factors. The influence can be depicted in Fig. 4. At the early stage of melt blending, as depicted in Fig. 4(a), UFPR particles mostly exist in aggregate form, while SBS phase exits in sphere form or in irregular shape. UFPR particles and SBS have no contact in PP matrix at this stage. With the progress of melt blending, UFPR particles and SBS begin to collide with each other under the shear force within the extruder, then most UFPR particles and SBS gradually combine together due to the driving force of compatibility. Since the solubility parameter of SBS is between those of UFPR and PP, SBS phase will distribute between UFPR and PP, and the encapsulation morphology with UFPR surrounded or partly surrounded by SBS is formed. SBS functions as the interface compatibilizer between the UFPR component and PP. The UFPR aggregates can be dispersed to form smaller aggregates or single particles with the help of SBS. After

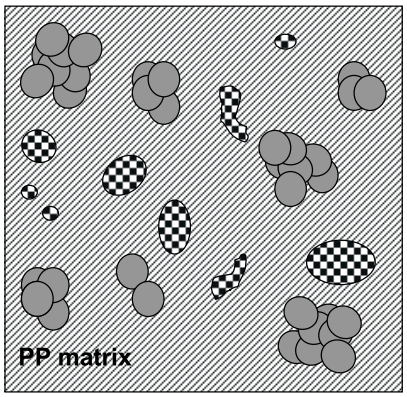

(a) at early stage of melt blending

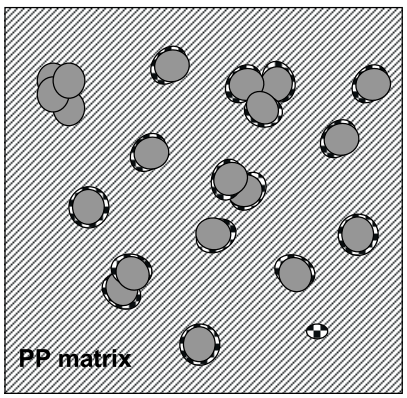

(b) after melt blending

Fig. 4. Schematic diagram depicting the morphology change of combined rubber system in PP matrix during melt blending process. The solid dark circle stands for the UFPR particle and the circle, ellipse and irregular shape filled with checker board represent the SBS phase.

melt blending the dispersion morphology is as depicted in Fig. 4(b). Since the UFPR component can disperse in smaller particle form, the number of rubber particles in unit volume of PP increases. The shear yielding of matrix and the energy absorption become easier under external force, which result in further increase of toughness, or the synergistic toughening effect.

4. Conclusion

Studied in this paper were the toughening effect of the UFPR/SBS combined rubber system on PP, the dispersion morphology of the rubber components in PP matrix, and their effect on crystallization behavior. The UFPR/SBS combined system has better toughening effect than the single rubber component. The UFPR compounded with nucleator has more prominent nucleation effect than SBS. It can increase the crystallinity of PP, and thus enhance the stiffness and heat resistance of PP. When UFPR was combined with a small amount of SBS, the strong nucleation ability can still be retained.

The UFPR/SBS combined rubber system exists in encapsulation morphology with UFPR surrounded or partly

surrounded by SBS in the PP matrix, and the incorporation of a small amount of SBS can help the dispersion of UFPR. Since the compatibility of SBS and PP is better than that of UFPR and PP, SBS can function as interface compatibilizer between UFPR and PP. It can help the UFPR aggregates to disperse better, therefore the number of rubber particles in PP matrix is increased, and the synergistic toughening effect is finally achieved.

Acknowledgements

This research was subsidized by the Special Funds for Major State Basic Research Projects G1999064800.

References

[1] Zhang M, Liu Y, Zhang X, Gao J, Huang F, Song Z, Wei G, Qiao J. Polymer 2002;43(19):5133–8.
[2] Liu Y, Zhang X, Wei G, Gao J, Huang F, Zhang M, Guo M, Qiao J. Chin J Polym Sci 2002;20(2):93–8.
[3] Huang F, Liu Y, Zhang X, Wei G, Gao J, Song Z, Zhang M, Qiao J. Macromol Rapid Commun 2002;23(13):786–90.
[4] Qiao J, Wei G, Zhang X, Zhang S, Gao J, Zhang W, Liu Y, Li J, Zhang F, Zhai R, Shao J, Yan K, Yin H. US Patent 6,423,760, July 23; 2002.
[5] Peng J, Qiao J, Zhang S, Wei G. Macromol Mater Engng 2002;287: 867–70.
[6] Peng J, Zhang X, Qiao J, Wei G. J Appl Polym Sci 2002;86(12): 3040–6.
[7] Zhang X, Wei G, Liu Y, Gao J, Zhu Y, Song Z, Huang F, Zhang M, Qiao J. Macromol Symp 2003;193:261–76.
[8] Jang BZ, Uhlmann DR, Vander Sande JB. J Appl Polym Sci 1985; 30(6):2485–504.
[9] Jang BZ, Uhlmann DR, Vander Sande JB. J Appl Polym Sci 1984; 29(13):4377–93.
[10] Karger-Kocsis J, Kallo A, Szafner A, Bodor G. Polymer 1979;20(1): 37–43.
[11] Stricker F, Thomann Y, Mulhaupt R. J Appl Polym Sci 1998;68(12): 1891–901.
[12] Yokoyama Y, Ricco T. Polymer 1998;39(16):3675–81.
[13] Wal A, Gaymans RJ. Polymer 1999;40(22):6067–75.
[14] Li Y, Wei GX, Sue HJ. J Mater Sci 2002;37(12):2447–59.
[15] Ou Y, Guo T, Fang X, Yu Z. J Appl Polym Sci 1999;74(10): 2397–403.
[16] Jancar J, Dibenedetto AT. J Mater Sci 1995;30(6):1601–8.
[17] Kolarik J, Jancar J. Polymer 1992;33(23):4961–7.
[18] Chiang WY, Yang WD, Pukanszky B. Polym Engng Sci 1992;32(10): 641–8.
[19] Long Y, Shanks RA. J Appl Polym Sci 1996;62(4):639–46.
[20] Pukanszky B, Tudos F, Kolarik J, Lednicky F. Polym Compos 1990; 11(2):98–104.
[21] Phadke AA, De SK. Polym Engng Sci 1986;26(15):1079–87.
[22] Fedors RF. Polym Engng Sci 1974;14(2):147–54.
[23] Van Krevelen DW. Properties of polymers. Their estimation and correlation with chemical structure. Amsterdam: Elsevier; 1976. Chapter 7.